AD

AD818491

TECHNICAL REPORT ECOM-01257-2

STUDY AND INVESTIGATION LEADING TO THE DESIGN OF BROADBAND HIGH POWER KLYSTRON AMPLIFIERS

SECOND TRI-ANNUAL REPORT

By

ERLING LIEN - DARRELL ROBINSON

JULY, 1967

ECOM

UNITED STATES ARMY ELECTRONICS COMMAND • FORT MONMOUTH, N.J. 07703

CONTRACT DA 28-043 AMC 02157(E)

EIMAC
DIVISION OF VARIAN
301 Industrial Way
San Carlos, California

NOTICES

DISCLAIMERS

The findings in this report are not to be construed as an official Department of the Army position, unless so designated by other authorized documents.

The citation of trade names and names of manufacturers in this report is not to be construed as official Government indorsement or approval of commercial products or services referenced herein.

DISPOSITION

Destroy this report when it is no longer needed. Do not return it to the originator.

TECHNICAL REPORT ECOM-02157-2 JULY, 1967

STUDY AND INVESTIGATION LEADING

to the

DESIGN OF BROADBAND HIGH-POWER KLYSTRON AMPLIFIERS

SECOND TRIANNUAL REPORT

10 December 1966 to 9 April 1967

Report No. 2

CONTRACT NO. DA 28-043 AMC-02157(E)

DA PROJECT NO. 1E6-22001-A-055-04-78

Prepared by

E. Lien and D. Robinson

EIMAC, Division of Varian

San Carlos, California

For

UNITED STATES ARMY ELECTRONICS COMMAND

Fort Monmouth, New Jersey 07703

ABSTRACT

The purpose of this program is to investigate methods for improving the bandwidth capabilities of high-power klystron amplifiers. The objective is a 1 db bandwidth improvement of at least fifty percent over the current state of the art. Particular emphasis is being placed on the study of extended-interaction resonators, and the possible optimization of these resonators through the use of mode overlapping.

In this report, the results of the continued investigation into the effects of mode overlapping in two-gap extended-interaction resonators are presented. An emphasis was placed on the study of the sensitivity of the resonator's frequency response to changes in the beam voltage, which seemed to be a major drawback of resonators with overlapping modes. It is shown that this sensitivity can be minimized by synchronizing the beam with the π mode. One theoretical example is cited wherein a beam voltage variation of more than fifty percent causes only small changes in the resonator's response and bandwidth.

Equations are derived for a computer program which will calculate the small-signal gain and phase response of klystrons employing extended-interaction resonators with overlapping modes. The gain equation is written in terms of the circuit admittance and electronic admittance matrices of each resonator, and the transfer admittance matrices between resonators. The equations were derived for the particular case of two-gap resonators, but the method is generally applicable to resonators with any number of gaps.

A cold-test method for use on extended-interaction resonators with overlapping modes, and on filter-loaded resonators, is developed theoretically. Through the use of this method, the elements of the impedance matrix of a resonator may be determined.

FOREWORD

This document is a report of the work performed on Contract DA 28-043 AMC-02157(E) during the second four-month period.

The program is being carried out in the High Power Microwave Tube Laboratory. The principal engineers are Erling Lien, who is serving as project leader, and Darrell Robinson.

Sponsorship and direction of the program are from the U.S. Army Electronics Command, Fort Monmouth, New Jersey. The assigned Army Project Engineer is Park Richmond.

TABLE OF CONTENTS

TABLE OF CONTENTS (Continued)

LIST OF FIGURES

INTRODUCTION

A. Purpose

The purpose of this program is to investigate methods for improving the bandwidth capabilities of high-power klystron amplifiers. The objective is a 1 db bandwidth improvement of at least fifty percent over the current state of the art. This is to be achieved without undue degradation of gain or efficiency and without sacrificing stability. Particular emphasis is being placed on the study of extended-interaction resonators, and the possible optimization of these resonators through the use of mode overlapping.

The investigation is being carried out theoretically with the aid of equivalent circuits and mathematical models, and experimentally to the extent of performing cold-test measurements on the resonators. Where applicable, resonator parameters are chosen to be consistent with a design example of a 5 megawatt peak-power klystron. Unless otherwise specified, the assumed parameters are the same as those listed in the Introduction section of the first triannual report of this contract.[1]

B. Progress

The major areas of progress in this contract during the second four-month reporting period were: the development of the working equations for a computer program which will calculate the small-signal performance of klystrons containing resonators with overlapping modes, and the theoretical study of cold-test methods applicable to such resonators. In addition, the investigation of the frequency response of two-gap resonators with mode overlap was

continued. Of particular interest this period was the minimization of the sensitivity of the resonators' frequency response to changes in the dc beam voltage.

Details of the progress in each of these areas are presented in the sections following.

FREQUENCY RESPONSE OF TWO-GAP RESONATORS WITH OVERLAPPING MODES

A. Introduction

The characteristics of two-gap resonators in which the two modes overlap in frequency were studied extensively during the previous reporting period. The results of this study were presented in the second section of the first triannual report of this contract[2]. Figures were included which illustrated the relationship between the frequency response of the resonators and combinations of the following parameters: the coupling between the two cavities, the degree of external loading of the cavities, the synchronization between the beam and the circuit, and the relative frequencies of the two cavities.

It was seen that for all but extreme coupling between the two cavities, the Q's of the two modes are approximately equal when the two cavities are tuned to the same frequency (equal frequencies before either cavity is externally loaded). In this case, the flattest response and maximum bandwidth is obtained when the beam is synchronized approximately midway between the two modes. If the two cavities are not tuned to the same frequency, the Q's of the two modes are definitely unequal. For example, if the loaded cavity is tuned low, the low-frequency mode has the lower Q, and the beam synchronization must favor that mode in order to have equal power output in both modes.

It was also noted that when the two cavities are tuned to the same frequency, the frequency response is quite sensitive to changes in the synchronization between the beam and the circuit. It will be shown in this section that this sensitivity can be greatly reduced by synchronizing the beam with the π mode. The loaded cavity is then

tuned low to optimize the response.

B. Minimizing the Sensitivity of the Frequency Response to Changes in the Beam Voltage

When a two-gap resonator with overlapping modes is excited by a modulated beam, the relative excitation of the two modes is dependent on both the parameters of the resonator and the synchronization of the beam with the modes. If the resonator parameters are chosen so the Q values of the two modes are equal, the beam must be synchronized approximately midway between them to excite them equally. If this condition exists, but then the beam synchronization changes (for example, because of a change in the dc beam velocity resulting from an increase or decrease in the dc beam voltage) one mode will be favored more than the other, causing a skewing of the resonator response with respect to frequency. This was illustrated for one particular case in Fig. 7 of the previous report[1], reproduced here as Fig. 1 for convenience. The two cavities of this resonator are assumed to be equal except for the external loading (equal values of resonant frequency, R_{sh}/Q, and Q for the two unloaded cavities). The beam synchronization is specified by the parameter θ_2, which is the phase angle between the rf currents exciting the two gaps. In the general case, these two currents are specified by the single drive-current vector

$$\underset{\sim}{I} = \begin{bmatrix} I_1 \\ I_2 \end{bmatrix} = A \begin{bmatrix} 1 \\ a_2 e^{j\theta_2} \end{bmatrix} \qquad (1)$$

where A and a_2 are real amplitude factors. a_2 is unity in the case of Fig. 1.

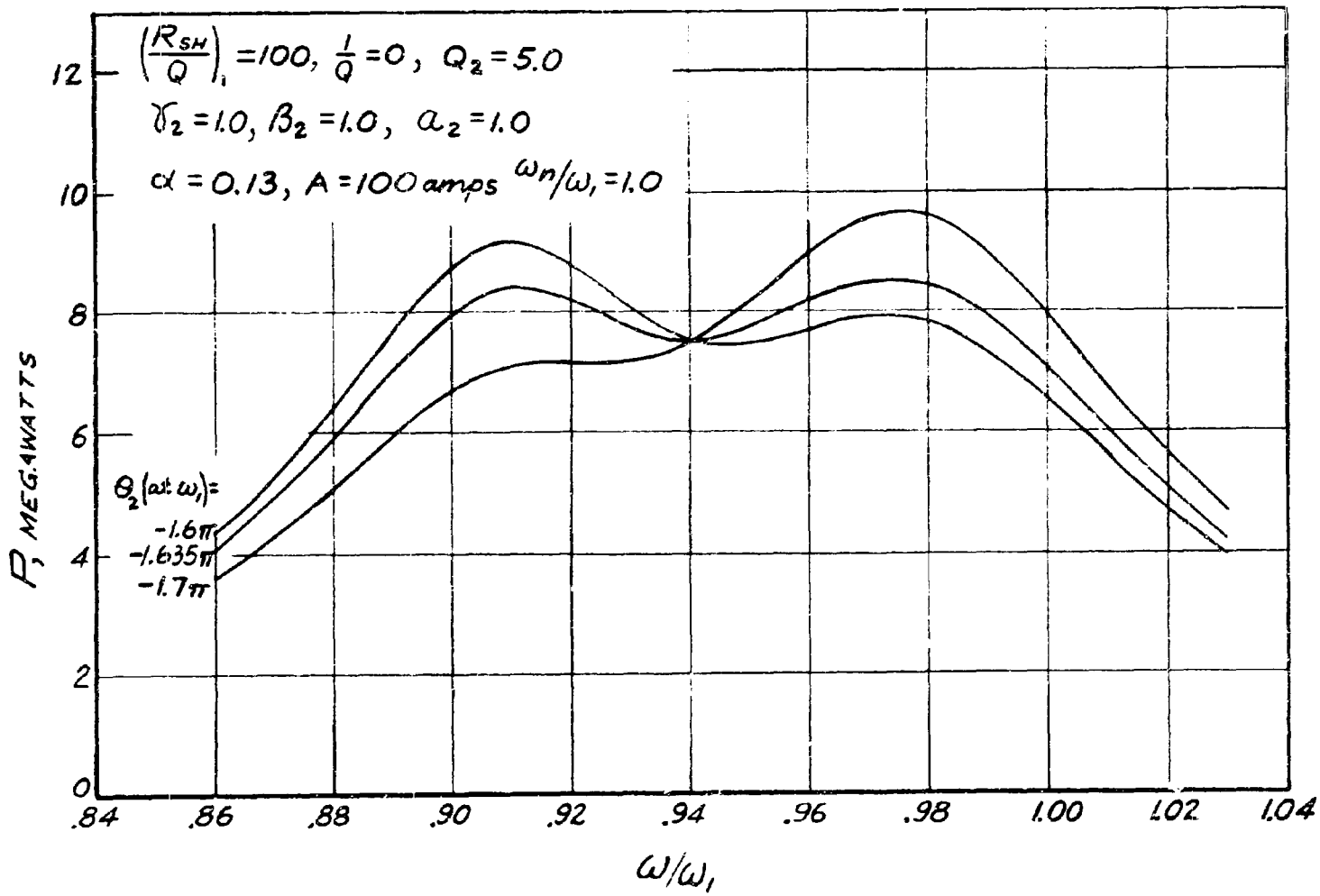

Fig. 1 - Resonator response curves showing the effect of changes in the beam synchronization. The two cavities are tuned to the same frequency, and the beam is synchronized approximately midway between the two modes.

The angle θ_2 represents the phase of the rf beam current at the second gap relative to the rf current at the first gap. When the rf gap voltages are small compared with the beam voltage, θ_2 is given by

$$\theta_2 \approx -\beta_e p \tag{2}$$

where p is the spacing between the gap centers and $\beta_e = \omega/u_o$ is the propagation factor associated with the dc beam velocity.

$\beta_e p$ represents the time phase delay caused by the dc drift of the electrons between the two gaps. For an output resonator, where appreciable energy extraction takes place in the first gap, the electrons will leave the gap with a velocity lower than the dc beam velocity. In this case,

$$\theta_2 < -\beta_e p \tag{3}$$

Any retardation of the beam current caused by the interaction in the first gap is presumed to be included in the value of θ_2. It can be seen from either Eq. (2) or (3) that θ_2 will be approximately proportional to frequency and to the inverse of the dc beam velocity when the spacing p remains constant.

Returning to the particular resonator under consideration, Fig. 1 shows that there is equal power output at the two modes when $\theta_2 = -1.63\pi$ (θ_2 is specified at ω_1, the resonant frequency of the unloaded and uncoupled first cavity of the resonator). The 1 db bandwidth for this case is 12.1 percent. If the value of θ_2 at the frequency ω_1 is changed to -1.6π, the lower-frequency mode (nominally the π mode) is favored more than the higher-frequency mode (nominally

the 2π mode) and the resulting 1 db bandwidth is slightly lower, being 11.0 percent.

When θ_2 (at ω_1) is changed to -1.7π, the higher-frequency mode is favored more than the other. This change in the beam synchronization is great enough to cause the maximum power output at the lower-frequency mode to be more than 1 db below the maximum power output at the upper mode. As a result, the 1 db bandwidth has been sharply reduced to only six percent. Thus it is seen that if this particular resonator were to be used in the output of a klystron, the maximum variation of the synchronization parameter θ_2 from the optimum value would have to be less than about four percent if the 1 db bandwidth were not to be greatly affected. With all other parameters fixed, this means that the maximum variation of the beam velocity from the optimum value would have to be less than about four percent.

It is useful to relate this percentage change in beam velocity to a corresponding change in the beam voltage. Including relativistic effects, the beam velocity and beam voltage are related by

$$eV_o = m_o c^2 \left[\frac{1}{\sqrt{1 - (u_o/c)^2}} - 1 \right] \tag{4}$$

where

V_o = dc beam voltage

u_o = dc beam velocity

e = charge of the electron

m_o = electron rest mass

c = free-space velocity of light

Letting

$$R_c = \frac{1}{\sqrt{1 - (u_o/c)^2}} \tag{5}$$

and solving Eq. (4) for R_c, we obtain

$$R_c = \frac{eV_o}{m_o c^2} + 1 \tag{6}$$

Solving Eq. (5) for u_o yields

$$u_o = c\sqrt{1 - (1/R_c)^2} \tag{7}$$

The rate of change of the beam velocity may be related to the rate of change of the beam voltage using Eq. (6), Eq. (7) and

$$\frac{du_o}{u_o} = \frac{1}{u_o} \frac{du_o}{dR_c} \frac{dR_c}{dV_o} dV_o \tag{8}$$

The result is

$$\frac{du_o}{u_o} = \frac{1}{R_c(R_c + 1)} \frac{dV_o}{V_o} \tag{9}$$

The quantity $1/R_c(R_c + 1)$ is plotted as a function of V_o in Fig. 2. The figure shows that the rate of change of beam velocity is approximately one half the rate of change of beam voltage at low voltages, and decreases as the voltage increases.

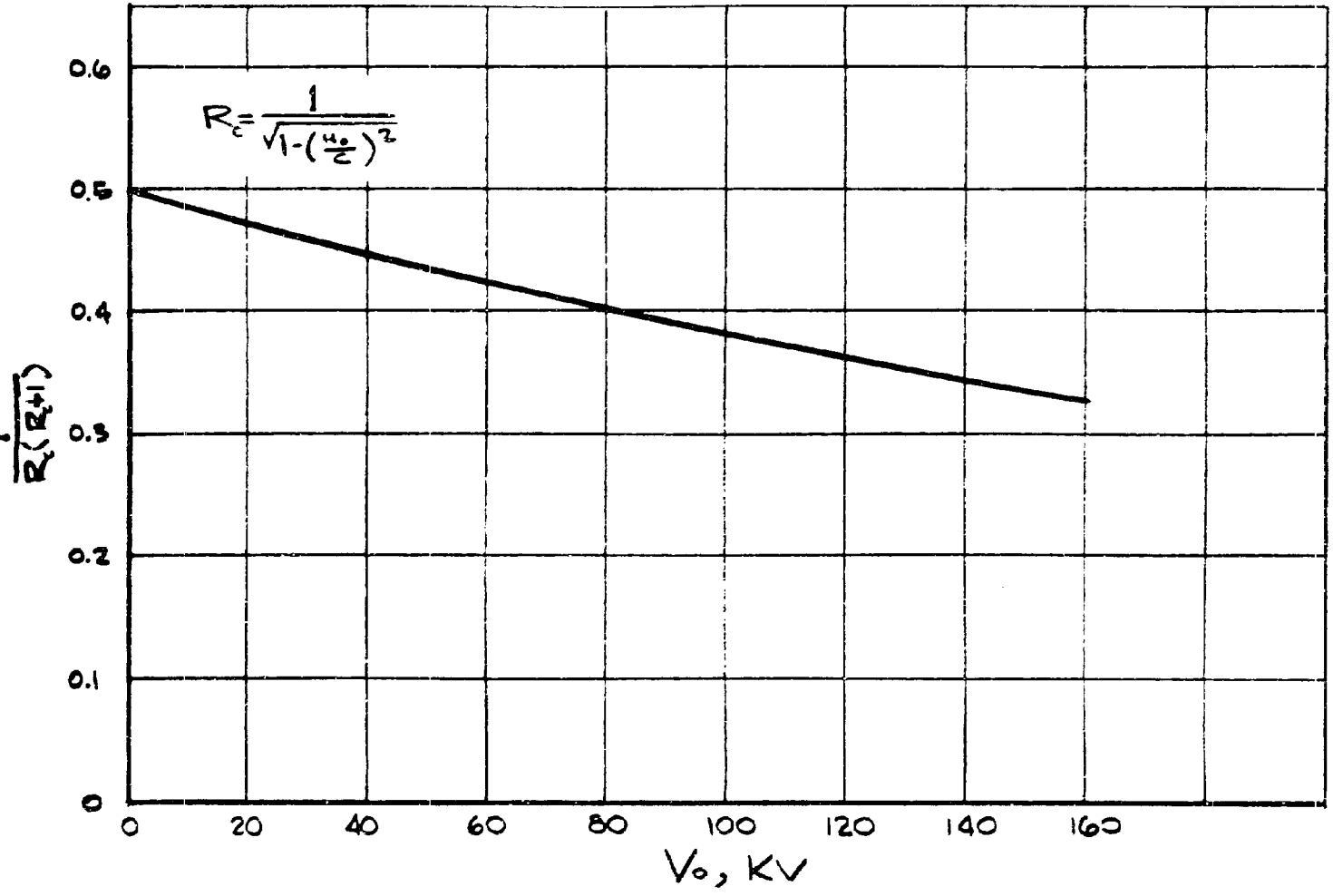

Fig. 2 - The function 1/R(R+1), relating the rate of change of beam velocity to the rate of change of beam voltage, versus beam voltage.

At V_o = 140 KV, where $1/R_c(R_c + 1) = 0.345$, a four percent change in the beam velocity corresponds to an 11.6 percent change in the beam voltage. This gives an approximate limit to the beam voltage variation that could be tolerated if the resonator of Fig. 1 were to be used as an output resonator and the 1 db bandwidth were not to be severely affected (assuming all other conditions were maintained constant). It should be noted that the range of variation of the operating beam voltage could be greater than the amount given above if one of the cavities of the resonator were made tunable. The change in the relative Q's of the two modes which would result from tuning one cavity could be used to compensate for the change in the beam synchronization.

The sensitivity of the resonator response to changes in the parameter θ_2 can be reduced from what it is in Fig. 1 by making use of the fact that the complex conjugate of a drive-current vector is equivalent to the original current vector as far as the power output of the resonator is concerned. That is, the power output at any given frequency will be unaltered if θ_2 is replaced by $-\theta_2$, with no other changes. (However, it was shown in the previous report that the gap voltages will be different, even though the output power is unchanged.)

In particular, the sensitivity of the response to changes in θ_2 can be minimized by synchronizing the beam with the π mode ($\theta_2 = -\pi$). If this is done, an increase in θ_2 due to a change in V_o will yield the same change in the output power at a given frequency as an equal decrease in θ_2 caused by an opposite change in V_o. This is true because the two resulting current vectors are complex conjugates of each other, as illustrated in Fig. 3. Note that the current I_1, used as a reference, is always real.

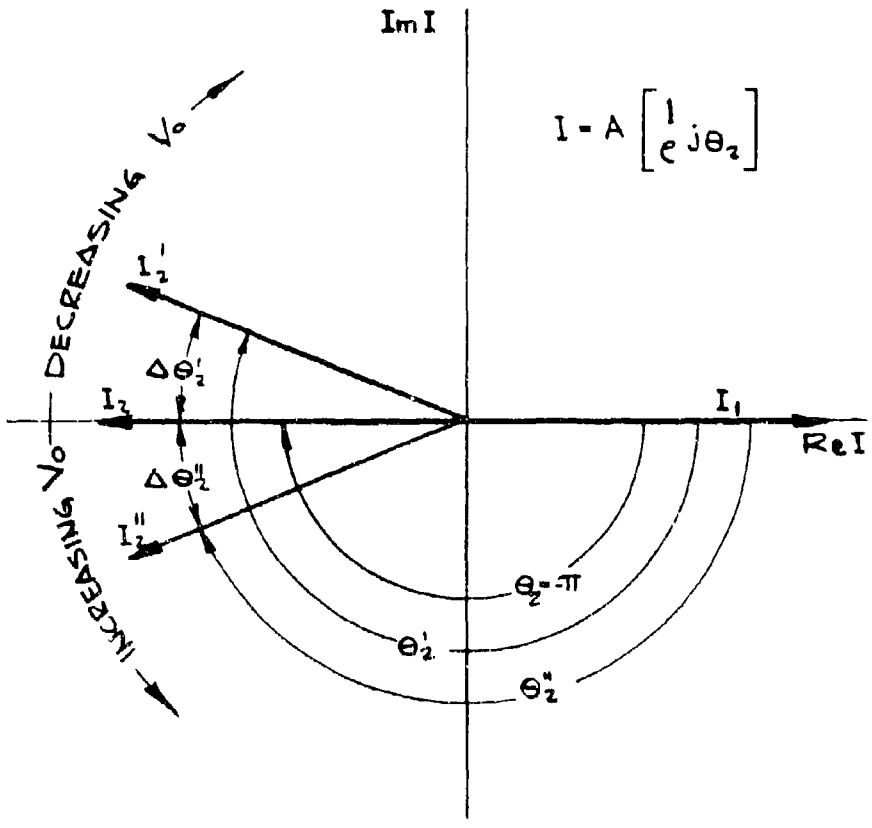

Fig. 3 - An illustration of how the drive current vector $\underset{\sim}{I}$ changes as the beam voltage varies from the value at which $\theta_2 = -\pi$. The frequency and gap-to-gap spacing are constant. When $\Delta\theta_2'' = \Delta\theta_2'$, $\underset{\sim}{I}'' = (\underset{\sim}{I}')^*$.

It should be pointed out that equal but opposite changes in θ_2 at one frequency will not produce the same effect on the output power over the entire frequency range of the response because of the frequency dependence of θ_2. When θ_2 is less than $-\pi$, θ_2 approaches $-\pi$, and the lower-frequency mode is favored more, as the frequency decreases. On the other hand when θ_2 is greater than $-\pi$, θ_2 recedes from $-\pi$, and the higher-frequency mode is favored more, as the frequency decreases. This is depicted in Fig. 4.

One example of the response of a resonator which is excited by a beam synchronized with the π mode was shown in Fig. 16 of the previous report[2]. That figure is reproduced here as the solid curve in Fig. 5. In this case, $\theta_2 = -\pi$ at the frequency of the lower mode, $\omega = 0.88\ \omega_1$ ($\theta_2 = -1.14\ \pi$ at ω_1). The loaded cavity (second cavity) has been tuned low by seven percent ($\gamma_2 = \omega_2/\omega_1 = 0.93$) to compensate for the beam synchronization and equalize the power output in the two modes.

The other curves of Fig. 5 illustrate the power response of this resonator for two other values of synchronization between the beam and the resonator ($\theta_2 = -.82\ \pi$ and $\theta_2 = -1.065\ \pi$ at $\omega = 0.88\ \omega_1$). The three response curves (and therefore also the bandwidth in the three cases) are nearly the same even though the phase angle θ_2 varies over a range of about 25 percent. Again assuming constant gap-to-gap spacing, this range of θ_2 corresponds to approximately a 25 percent variation of the beam velocity, which in turn corresponds to a beam voltage variation of over 50 percent. Thus it is seen that by a proper choice of the beam synchronization, it is possible to operate a two-gap resonator with mode overlap over a wide range of dc beam voltages without seriously affecting its power response or bandwidth.

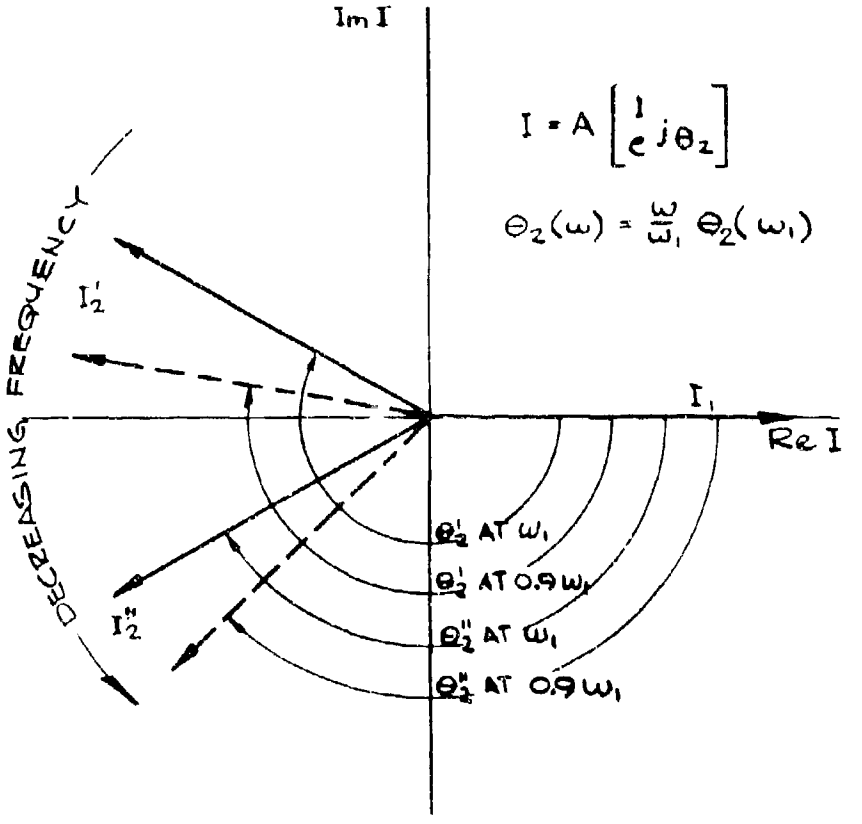

Fig. 4 - An illustration of how the drive current vectors $\underset{\sim}{I}'$ and $\underset{\sim}{I}''$ vary with frequency. The beam voltage and gap-to-gap spacing are constant.

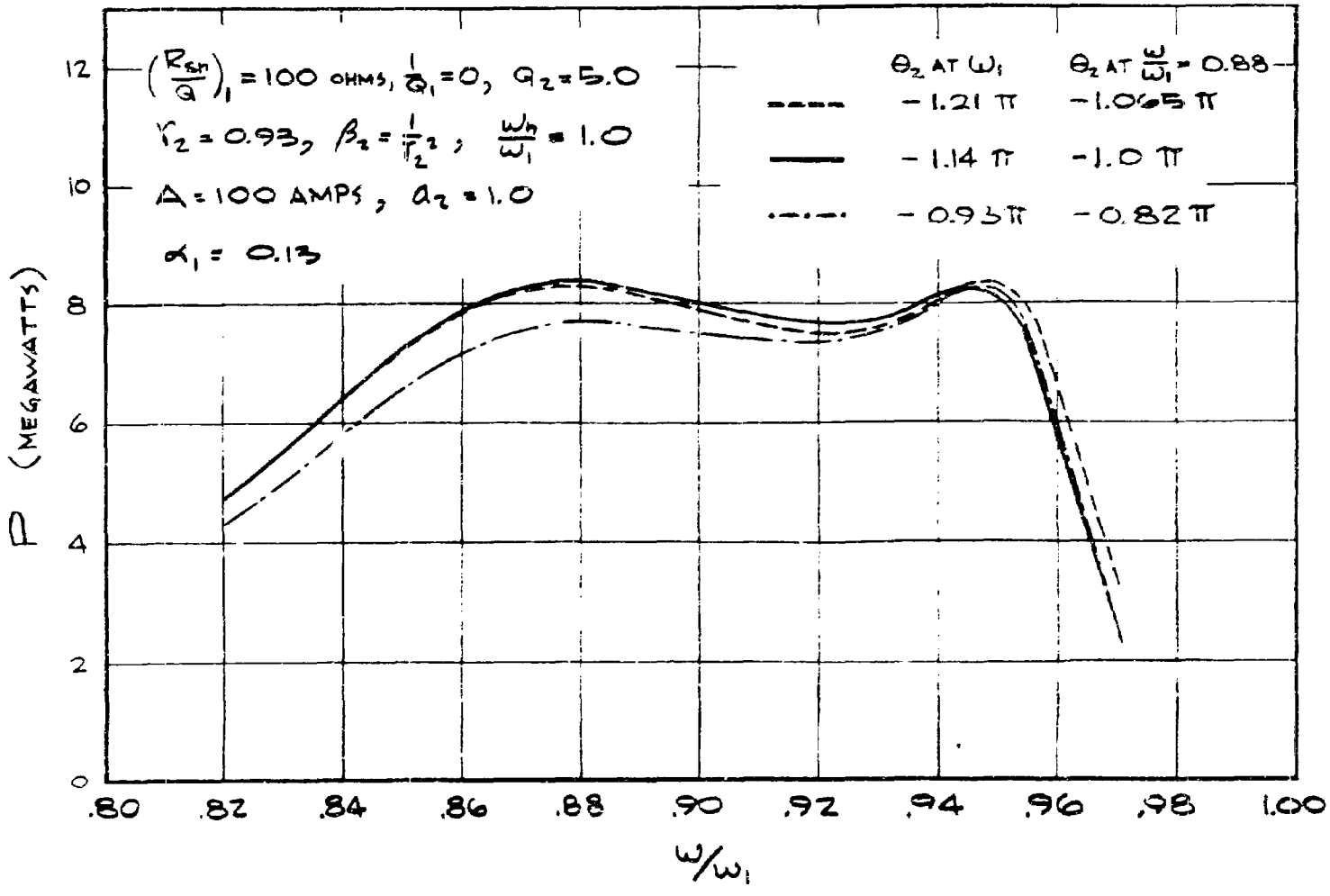

Fig. 5 - Resonator response curves showing the effect of changes in the beam synchronization. The loaded cavity is tuned low, and the beam is synchronized with the π mode at $\omega/\omega_1 = 0.88$ (solid curve).

SMALL-SIGNAL GAIN-BANDWIDTH RESPONSE OF KLYSTRONS WITH MODE-OVERLAPPING RESONATORS

A. Introduction

A computer program is being written to calculate the small-signal gain and phase response of klystrons which employ extended-interaction resonators with overlapping modes. The equations used in the program have been derived and are based on the small-signal theory of Wessel-Berg[3]. This theory is a one-dimensional space-charge-wave theory of the interaction between a longitudinal beam and an amplifier structure composed of a number of adjacent but uncoupled interaction regions of arbitrary lengths and arbitrary rf field distributions. Wessel-Berg's theory is non-relativistic, but relativistic effects are being taken into account in the computer program by using corrected values of beam velocity, coupling coefficients, beam-loading conductance, and plasma frequency. The relativistic corrections being applied to these parameters were described in the first quarterly report of a previous contract[4].

The method being used to compute the gain and phase response of klystrons employing mode-overlapping resonators follows closely the method of Wessel-Berg for calculating the response of klystrons composed of a number of cavity groups[5]. In our case one extended-interaction resonator, consisting of a number of single-gap cavities coupled to each other and to the beam but not coupled to the cavities of any other resonator except through the beam, is analogous to a cavity group. (An isolated single-gap cavity can be considered a special case of a cavity group.) The gain equation for the overall klystron is written

in terms of the circuit and electronic matrices of each resonator, and the matrices describing the transfer admittance between the resonators.

The computer program is being restricted to klystrons with only two-gap extended-interaction resonators and conventional single-gap resonators. However, the method is equally applicable to klystrons containing resonators with any number of gaps, including multiple-tuned single-gap resonators.

The development of the equations for the computer program can be divided into three general phases: relating the output resonator gap voltages to the input resonator gap voltages, relating the input resonator gap voltages to the power available from the generator, and relating to output power delivered to the load to the output resonator gap voltages. These three phases are discussed separately below.

B. Relating the Output Resonator Gap Voltages to the Input Resonator Gap Voltages

Consider the klystron shown schematically in Fig. 6, consisting of p inductively-coupled two-gap resonators. Let each resonator be represented by the equivalent circuit of Fig. 7, applied specifically here to the sth resonator. Each cavity of the resonator is represented as a series R-L-C circuit, and the coupling between the two cavities is simulated by the shunt inductance L_o. The resistance R in each cavity includes losses due to external loading of the cavity and resistance in the cavity walls. For a more complete discussion of the characteristics of this equivalent circuit see reference 2.

The subscript notation used in the preceding two figures, and to be used in this section of the report, is as follows. When two subscripts appear together with no separating comma, the first refers to

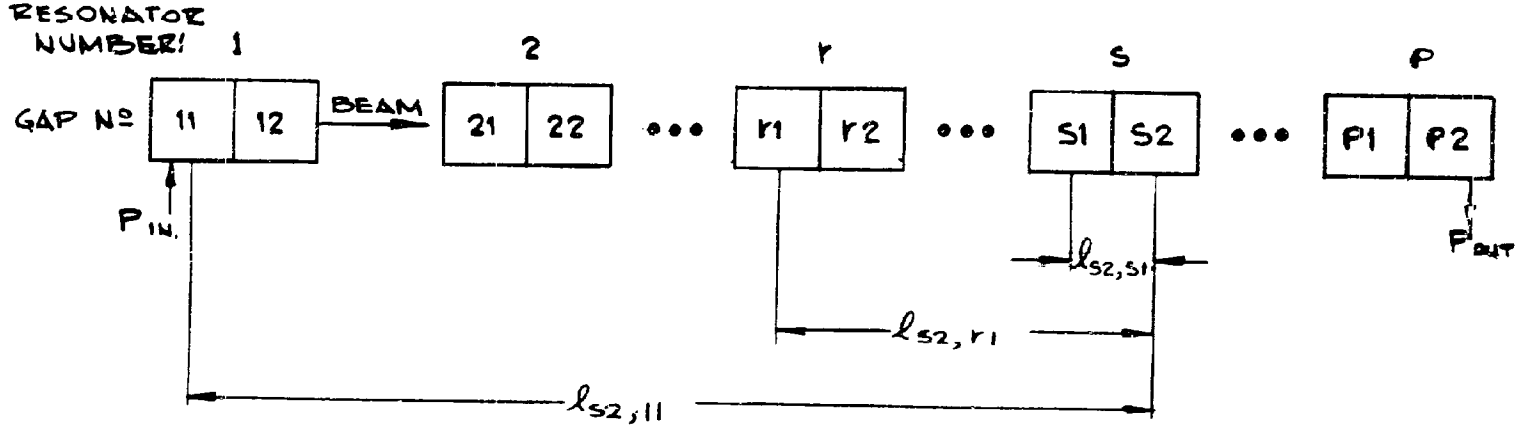

Fig. 6 - Schematic drawing of a klystron containing p two-gap resonators.

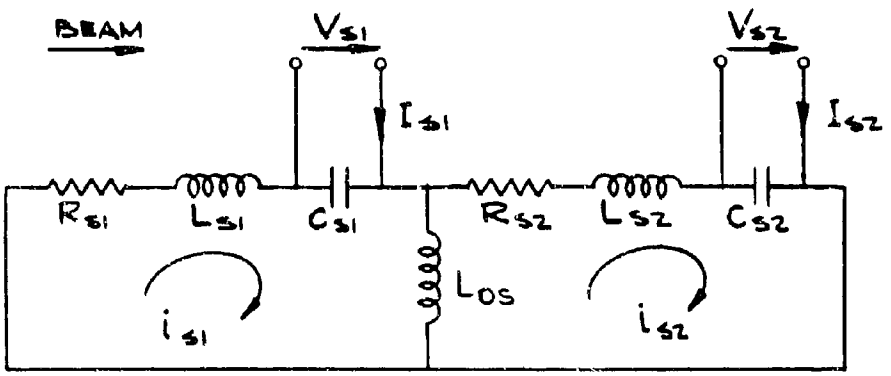

Fig. 7 - Equivalent circuit for the sth two-gap, inductively-coupled resonator of the klystron shown schematically in Fig. 6.

the resonator number and the second to the number of the gap within the resonator. When the gaps of two different resonators are involved, the subscript pairs appear with a comma between. If two single subscripts are separated by a comma, both refer to resonator numbers.

Wessel-Berg has shown[5] that the relationship between the rf gap voltages in the pth resonator and the rf gap voltages in the first resonator can be written as the following determinant of matrices:

$$\underset{\sim}{V}_p = \begin{vmatrix} \underset{\sim}{1} & \underset{\sim}{0} & \underset{\sim}{0} & \cdot & \cdot & \underset{\sim}{V}_1 \\ -\underset{\sim}{\eta}_{2,1} & \underset{\sim}{1} & \underset{\sim}{0} & \cdot & \cdot & \underset{\sim}{0} \\ -\underset{\sim}{\eta}_{3,1} & -\underset{\sim}{\eta}_{3,2} & \underset{\sim}{1} & \cdot & \cdot & \underset{\sim}{0} \\ \cdot & \cdot & \cdot & \cdot & \cdot & \cdot \\ \cdot & \cdot & \cdot & \cdot & \cdot & \cdot \\ -\underset{\sim}{\eta}_{p,1} & -\underset{\sim}{\eta}_{p,2} & -\underset{\sim}{\eta}_{p,3} & \cdot & -\underset{\sim}{\eta}_{p,p-1} & \underset{\sim}{0} \end{vmatrix} \tag{10}$$

where

$$\underset{\sim}{V}_p = \begin{bmatrix} V_{p1} \\ V_{p2} \end{bmatrix} \tag{11}$$

and

$$\underset{\sim}{V}_1 = \begin{bmatrix} V_{11} \\ V_{12} \end{bmatrix} \tag{12}$$

Except for $\underset{\sim}{V}_1$, all of the elements of the determinant in Eq. (10) are two-by-two matrices (in the case of two-gap resonators). The values of the elements of $\underset{\sim}{V}_p$ are found by expanding the determinant using standard rules. However, care must be taken to multiply the

matrices together in the correct order (terms with the highest indices should appear first).

The η matrices in the determinant are given by

$$\underset{\sim}{\eta}_{s,r} = - \underset{\sim}{Y}_{s,s}^{-1} \underset{\sim}{Y}_{s,r} \tag{13}$$

where $\underset{\sim}{Y}_{s,s}$ is the self-admittance matrix associated with the sth resonator, and $\underset{\sim}{Y}_{s,r}$ is the transfer admittance matrix between the rth and the sth resonators. Note that s will range from 2 to p while r will range from 1 to p-1 (s will always be greater than r). The matrix $\underset{\sim}{\eta}_{s,r}$ represents the voltage-gain matrix of a klystron consisting of only the resonators r and s.

The self-admittance matrix $\underset{\sim}{Y}_{s,s}$ is the sum of the circuit admittance and electronic admittance matrices of the resonator s:

$$\underset{\sim}{Y}_{s,s} = \underset{\sim}{Y}_{c,s} + \underset{\sim}{Y}_{e,s} \tag{14}$$

The circuit admittance matrix is just the inverse of the circuit impedance matrix, described in detail in Appendix I of Reference 1:

$$\underset{\sim}{Y}_{c,s} = Z_{c,s}^{-1} \tag{15}$$

The electronic admittance matrix is given by

$$\underset{\sim}{Y}_{e,s} = \begin{bmatrix} Y_{e,s1} & 0 \\ Y_{s2,s1} & Y_{e,s2} \end{bmatrix} \tag{16}$$

where $Y_{e,sn}$ is the beam loading admittance of the nth gap, and $Y_{s2,s1}$ is the electronic transfer admittance from first to the second gap.

The susceptive part of the beam loading of any one gap can be included in the equivalent-circuit capacitance of that gap. If this is done, the matrix $\underset{\sim}{Y}_{e,s}$ can be written

$$\underset{\sim}{Y}_{e,s} = \begin{bmatrix} G_{e,s1} & 0 \\ Y_{s2,s1} & G_{e,s2} \end{bmatrix} \tag{17}$$

where $G_{e,sn}$ is the real part of $Y_{e,sn}$, or the beam loading conductance of the nth gap. The expression for this conductance is

$$G_{e,sn} = \frac{1}{8} \frac{I_o}{V_o} \frac{\omega}{\omega_q} \left[\left| M_{sn}^{-} \right|^2 - \left| M_{sn}^{+} \right|^2 \right] \tag{18}$$

where

$$M_{sn}^{-} = M_{sn}(\beta_e - \beta_q) \tag{19}$$

is the coupling coefficient of the fast space-charge wave, and

$$M_{sn}^{+} = M_{sn}(\beta_e + \beta_q) \tag{20}$$

is the coupling coefficient of the slow space-charge wave.

The electronic transfer admittance $Y_{s2,s1}$ between the first and second gaps of the sth resonator is given by

$$Y_{s2,s1} = \frac{1}{4} \frac{I_o}{V_o} \frac{\omega}{\omega_q} \left[M_{s2}^{-} M_{s1}^{-} e^{-j(\beta_e - \beta_q) \ell_{s2,s1}} - M_{s2}^{+} M_{s1}^{+} e^{-j(\beta_e + \beta_q) \ell_{s2,s1}} \right] \tag{21}$$

The matrix $\underset{\sim}{Y}_{s,r}$, expressing the transfer admittance from the rth resonator to the sth resonator, is the matrix

$$\underset{\sim}{Y}_{s,r} = \begin{bmatrix} Y_{s1,r1} & Y_{s1,r2} \\ Y_{s2,r1} & Y_{s2,r2} \end{bmatrix} \tag{22}$$

where

$$Y_{sn,rm} = \frac{1}{4} \frac{I_o}{V_o} \frac{\omega}{\omega_q} \left[M_{sn}^{-} M_{rm}^{-} e^{-j(\beta_e - \beta_q)\ell_{sn,rm}} - M_{sn}^{+} M_{rm}^{+} e^{-j(\beta_e + \beta_q)\ell_{sn,rm}} \right] \tag{23}$$

The expressions given above were derived for the situation where all of the resonators in the klystron are two-gap resonators. However, they are also applicable when one or more single-gap resonators are included in the tube. In this case, the coupling coefficients of one of the gaps and the inductance L_o in the equivalent circuit (Fig. 7) are set equal to zero for each single-gap resonator involved.

C. Relating the Input Resonator Gap Voltages to the Available Generator Power

If the generator is coupled to the first cavity of the two-gap input resonator, the equivalent circuit of the resonator-generator combination will be as shown in Fig. 8. As before, the resistance in each cavity includes the losses in the cavity wall and any external loading of the cavity (but does not include the coupling to the generator). The generator is represented as a constant-voltage source V_g in series with an effective internal impedance R_g (real).

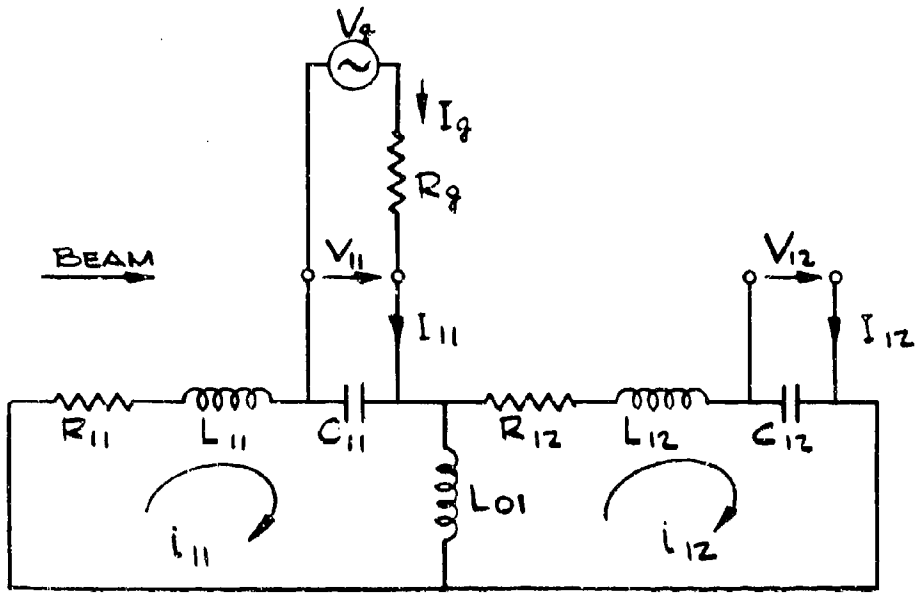

Fig. 8 - Equivalent circuit of the two-gap input resonator showing the generator coupled to the first cavity.

The generator could also be coupled to the second cavity of the resonator. In either case, the gap voltages V_{11} and V_{12} can be related to the current excitation of the resonator through the matrix equation

$$\underset{\sim}{V}_1 = \underset{\sim}{Y}_{1,1}^{-1} \underset{\sim}{I}_1 \tag{24}$$

where $\underset{\sim}{Y}_{1,1}$ is the self-admittance matrix of the resonator. $\underset{\sim}{V}_1$ is the gap-voltage vector (Eq. (12)), and $\underset{\sim}{I}_1$ is the induced-current vector of the resonator. $Y_{1,1}$ is the sum of the circuit and electronic admittance matrices:

$$\underset{\sim}{Y}_{1,1} = \underset{\sim}{Y}_{c,1} + \underset{\sim}{Y}_{e,1} \tag{25}$$

$\underset{\sim}{Y}_{c,1}$ and $\underset{\sim}{Y}_{e,1}$ are found from Eqs. (15) and (17), respectively, with $s = 1$. The real part of the beam-loading admittances of the two gaps are represented by the diagonal elements of the $\underset{\sim}{Y}_{e,1}$ matrix, while the beam transfer admittance is represented by the off-diagonal element $Y_{12,11}$.

Letting $\underset{\sim}{Y}_{1,1}^{-1} = \underset{\sim}{Z}_{1,1}$, and writing Eq. (24) in terms of its components, we have

$$\begin{bmatrix} V_{11} \\ V_{12} \end{bmatrix} = \begin{bmatrix} Z_{11,11} & Z_{11,12} \\ Z_{12,11} & Z_{12,12} \end{bmatrix} \begin{bmatrix} I_{11} \\ I_{12} \end{bmatrix} \tag{26}$$

Since the beam loading of the individual gaps and the excitation of the second cavity by the rf modulation on the beam are included in the elements of the matrix $\underset{\sim}{Z}_{1,1}$, the currents I_{11} and I_{12} include only excitation from external sources. Thus when the generator is coupled to the first cavity, $I_{11} = I_g$ and $I_{12} = 0$. If the generator is coupled

to the second cavity, $I_{11} = 0$ and $I_{12} = I_g$. Given the elements of the $\underset{\sim}{Z}_{1,1}$ matrix, the gap voltages can be completely determined once the gap to which the generator is coupled has been specified and the current I_g has been related to the generator power.

The power which is available from the generator is the power delivered to the resonator when its input impedance, as seen by the generator, is real and equal to R_g. It is given by

$$P_a = \frac{1}{8} \frac{V_g V_g^*}{R_g} \tag{27}$$

This equation gives only the magnitude of V_g in terms of the available power. Let the phase of V_g be chosen as a reference and set equal to zero. Then

$$V_g = \sqrt{8 R_g P_a} \tag{28}$$

The current I_g will be

$$I_g = \frac{V_g}{R_g + Z_i} \tag{29}$$

where Z_i, the input impedance as seen by the generator, is defined to be

$$Z_i = \frac{V_{1n}}{I_g} \tag{30}$$

The subscript n refers to the number of the gap to which the generator is coupled.

In general, the gap voltages will be dependent on whether the generator is coupled to the first cavity or the second. These two cases are discussed separately below. However, note that in either case the input voltage standing-wave ratio S can be computed, once Z_i is known, from

$$S = \frac{1 + |\rho|}{1 - |\rho|} \tag{31}$$

where ρ, the voltage reflection coefficient, is

$$\rho = \frac{Z_i - R_g}{Z_i + R_g} \tag{32}$$

1. Generator Coupled to the First Cavity

When the generator is coupled to the first cavity, $I_{11} = I_g$ and $I_{12} = 0$. Substituting these values into Eq. (26) and expanding yields the two equations

$$V_{11} = Z_{11,11} I_g \tag{33}$$

$$V_{12} = Z_{12,11} I_g \tag{34}$$

Comparing Eq. (33) with Eq. (30), we see that

$$Z_i = Z_{11,11} \tag{35}$$

Combining Eqs. (28), (29), (33), and (35), we obtain

$$V_{11} = \frac{Z_{11,11}}{R_g + Z_{11,11}} \sqrt{8 R_g P_a} \tag{36}$$

This equation relates the rf voltage at the first gap to the available generator power when the generator is coupled to the first cavity. The voltage at the second gap is then found from Eqs. (33) and (34):

$$V_{12} = \frac{Z_{12,11}}{Z_{11,11}} V_{11} \tag{37}$$

In this case, the effective internal impedance of the generator is given by

$$R_g = (R_{sh}/Q)_{11} (Q_{ext})_{g,11} \tag{38}$$

where $(Q_{ext})_{g,11}$ is the external Q of the first cavity associated with the coupling to the generator.

2. Generator Coupled to the Second Cavity

When the generator is coupled to the second cavity, $I_{11} = 0$ and $I_{12} = I_g$. Substituting these values of current into Eq. (26), we obtain

$$V_{11} = Z_{11,12} I_g \tag{39}$$

$$V_{12} = Z_{12,12} I_g \tag{40}$$

From Eqs. (30) and (40), the input impedance Z_i is

$$Z_i = Z_{12,12} \tag{41}$$

Combining Eqs. (39), (40), and (41) with Eqs. (28) and (29) yields

$$V_{12} = \frac{Z_{12,12}}{R_g + Z_{12,12}} \sqrt{8 R_g P_a} \tag{42}$$

and

$$V_{11} = \frac{Z_{11,12}}{Z_{12,12}} V_{12} \tag{43}$$

These last two equations define the elements of gap voltage vector $\underset{\sim}{V}_1$ when the generator is coupled to the second cavity. The effective internal impedance of the generator in this case is

$$R_g = (R_{sh}/Q)_{12} (Q_{ext})_{g,12} \tag{44}$$

where $(Q_{ext})_{g,12}$ is the external Q of the second cavity associated with the coupling to the generator.

D. Klystron Output Power, Gain, and Phase Shift

The average rf power delivered from the beam to the pth (output) resonator can be found from the voltage matrix and the circuit admittance matrix of that resonator. The relationship is

$$P_p = \frac{1}{2} R_e \left[\tilde{V}_p^* \underset{\sim}{Y}_{c,p} \underset{\sim}{V}_p \right] \tag{45}$$

where $\tilde{V}_p$ is the transpose of the voltage matrix $\underset{\sim}{V}_p$ and the asterisk indicates complex conjugate. If the losses in the cavity walls are negligible and there is only one external load coupled to the

resonator, essentially all of the power delivered to the resonator will be dissipated in the load. In this case,

$$P_{out} = P_p \tag{46}$$

The power gain of the klystron, in decibels, will be given by

$$\text{Gain} = 10 \log_{10} \frac{P_{out}}{P_a} \tag{47}$$

The phase shift ϕ through the tube is defined to be:

$$\phi = \tan^{-1} \left(\frac{V_{pn}}{V_g}\right) \tag{48}$$

where n refers to the number of the cavity within the pth resonator to which the load is coupled.

MEASUREMENT METHOD FOR COLD TEST OF EXTENDED-INTERACTION RESONATORS HAVING MODE OVERLAPPING

A. Introduction

The theoretical basis for cold-test techniques applicable to extended-interaction resonators with mode overlapping was developed during the second reporting period and is described in this section.

Standard cold-test procedures used for single-mode resonators do not provide sufficient information for predicting the performance of resonators with mode overlapping. A single-mode resonator is normally represented by an equivalent circuit having a single resonant element. Only two parameters, the (R_{sh}/Q) and the loaded-Q factor, are required for the calculation of the interaction impedance and the frequency response of this resonator. The goals of standard resonator cold-test techniques are to determine the (R_{sh}/Q) and the loaded-Q factor.

The representation of the resonator performance becomes more complex when mode overlapping is allowed. In this case it is convenient to use circuit impedance matrices to express the relations between the voltages and induced currents in the interaction gaps. The circuit impedance matrix is completely defined when the values of all its elements are known as a function of frequency. Methods have been derived whereby the elements of the resonator's impedance matrix may be determined. The values of the transfer elements of the matrix (off-diagonal elements), relative to one or more of the self-impedance elements of the gaps, can be evaluated by exciting each cavity sequentially with small coupling loops and measuring the change in the transmission (magnitude and phase) to the load port when the gaps

are perturbed. The self impedance of each gap, relative to the self impedance of a reference gap, may also be measured in this manner. The method is described in part B of this section. The self impedance of each gap may be determined by exciting the resonator at the load port and measuring the change in the reflection coefficient as each gap is perturbed. This method is described in part C of this section.

B. Measurement of the Circuit Matrix Elements by Capacitive Perturbation of the Interaction Gaps

In the derivation of the theoretical basis for the measurement method, the equivalent lumped circuit model shown in Fig. 9 is used to represent the actual coupled-cavity extended-interaction resonator.

The extended-interaction resonator consists of n coupled resonators. For simplicity we will assume that all the interaction gaps have equal capacitances. This will be true for most resonator designs. The other circuit elements may vary from cell to cell.

We shall first define the appropriate variables to be used in the analysis and derive their interrelations.

We shall define a gap voltage vector $\underset{\sim}{V}$

$$\underset{\sim}{V} = \begin{bmatrix} V_1 \\ V_2 \\ \vdots \\ V_p \\ \vdots \\ V_n \end{bmatrix} \tag{49}$$

and similarly vectors describing the driving currents I in the interaction gaps and the mesh currents i:

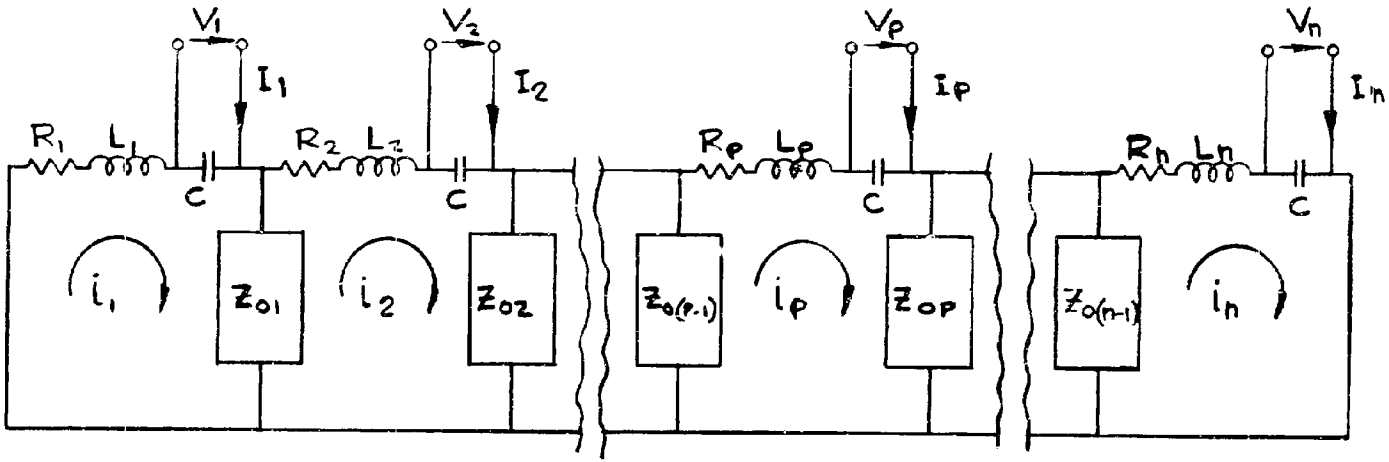

Fig. 9 - Equivalent lumped circuit consisting of n coupled resonators. The individual resonator cells have identical interaction gap capacitances.

$$\underset{\sim}{i} = \begin{bmatrix} i_1 \\ i_2 \\ \vdots \\ i_p \\ \vdots \\ i_n \end{bmatrix} \quad , \qquad \underset{\sim}{I} = \begin{bmatrix} I_1 \\ I_2 \\ \vdots \\ I_p \\ \vdots \\ I_n \end{bmatrix} \tag{50}$$

Applying Kirchhoff's laws to the circuit and writing the resulting equations in matrix form, we obtain

$$\underset{\sim}{K}\,\underset{\sim}{i} = \underset{\sim}{C}\,\underset{\sim}{I} \tag{51}$$

where

$$\underset{\sim}{C} = \frac{1}{j\omega C}\,\underset{\sim}{1} \tag{52}$$

and $\underset{\sim}{1}$ is the unity matrix. The mesh impedance matrix $\underset{\sim}{K}$ is given by:

$$\underset{\sim}{K} = \begin{bmatrix} (Z_1 + Z_{o1}) & -Z_{o1} & 0 & \cdots & 0 \\ -Z_{o1} & (Z_2 + Z_{o1} + Z_{o2}) & -Z_{o2} & \cdots & 0 \\ \vdots & \ddots & \ddots & \ddots & \vdots \\ 0 & \cdots & -Z_{o(p-1)} & (Z_p + Z_{o(p-1)} + Z_{op}) & -Z_{op} \\ \vdots & \ddots & \ddots & \ddots & \vdots \\ 0 & \cdots & 0 & -Z_{o(n-1)} & (Z_n + Z_{o(n-1)}) \end{bmatrix} \tag{53}$$

where

$$Z_p = R_p + j\left(\omega L_p - \frac{1}{\omega C}\right) \tag{54}$$

The gap voltages are given by

$$\underset{\sim}{V} = \underset{\sim}{C}\left(\underset{\sim}{I} - \underset{\sim}{i}\right) \tag{55}$$

Combining Eqs. (51) and (55) we obtain:

$$\underset{\sim}{V} = \underset{\sim}{C}\,\underset{\sim}{I} - \underset{\sim}{C}\,\underset{\sim}{K}^{-1}\,\underset{\sim}{C}\,\underset{\sim}{I} \tag{56}$$

We have defined the circuit matrix $\underset{\sim}{Z}_c$ to be

$$\underset{\sim}{Z}_c = \underset{\sim}{C} - \underset{\sim}{C}\,\underset{\sim}{K}^{-1}\,\underset{\sim}{C} \tag{57}$$

which yields the relationship

$$\underset{\sim}{V} = \underset{\sim}{Z}_c\,\underset{\sim}{I} \tag{58}$$

The change $(d\underset{\sim}{Z}_c)$ in the circuit matrix produced by a perturbation of one of the circuit elements (for example the capacitance C of the pth interaction gap) is given by

$$(d\underset{\sim}{Z}_c) = (d\underset{\sim}{C}) - (d\underset{\sim}{C})\,\underset{\sim}{K}^{-1}\,\underset{\sim}{C} - \underset{\sim}{C}\,(d\underset{\sim}{K}^{-1})\,\underset{\sim}{C} - \underset{\sim}{C}\,\underset{\sim}{K}^{-1}\,(d\underset{\sim}{C}) \tag{59}$$

We do not have any explicit expression for the inverted mesh impedance matrix $\underset{\sim}{K}^{-1}$ and must eliminate this matrix from Eq. (59).

From the relation

$$\underset{\sim}{K}\,\underset{\sim}{K}^{-1} = \underset{\sim}{1} \tag{60}$$

we obtain

$$(d\underset{\sim}{K})\,\underset{\sim}{K}^{-1} + \underset{\sim}{K}\,(d\underset{\sim}{K}^{-1}) = 0 \tag{61}$$

Therefore

$$(d\underset{\sim}{K}^{-1}) = -\,\underset{\sim}{K}^{-1}\,(d\underset{\sim}{K})\,\underset{\sim}{K}^{-1} \tag{62}$$

Combining Eqs. (59) and (62) and making use of Eq. (57) we obtain

$$(d\underset{\sim}{Z}_c) = -\,(d\underset{\sim}{C}) + (d\underset{\sim}{K}) + (d\underset{\sim}{C})\,\underset{\sim}{C}^{-1}\,\underset{\sim}{Z}_c + \underset{\sim}{Z}_c\,\underset{\sim}{C}^{-1}\,(d\underset{\sim}{C})$$

$$-\underset{\sim}{Z}_c\,\underset{\sim}{C}^{-1}(d\underset{\sim}{K}) - (d\underset{\sim}{K})\underset{\sim}{C}^{-1}\,\underset{\sim}{Z}_c + \underset{\sim}{Z}_c\,\underset{\sim}{C}^{-1}\,d\underset{\sim}{K}\,\underset{\sim}{C}^{-1}\,\underset{\sim}{Z}_c \tag{63}$$

We shall define a matrix $\underset{\sim}{P}$ having all elements equal to zero except for the pth diagonal element which is unity. For a perturbation of the susceptance $d(\omega C)$ of the pth gap we see from Eq. (52) that

$$(d\underset{\sim}{C}) = -\,\frac{d(\omega C)}{j(\omega C)^2}\,\underset{\sim}{P} \tag{64}$$

Similarly from Eqs. (53) and (54) we see that

$$(d\underset{\sim}{K}) = -\,\frac{d(\omega C)}{j(\omega C)^2}\,\underset{\sim}{P} \tag{65}$$

Therefore

$$(d\underset{\sim}{C}) = (d\underset{\sim}{K}) \tag{66}$$

Combining Eqs. (59) and (66) we get

$$(d\underset{\sim}{Z}_c) = \underset{\sim}{Z}_c \, \underset{\sim}{C}^{-1} \, (d\underset{\sim}{K}) \, \underset{\sim}{C}^{-1} \, \underset{\sim}{Z}_c \tag{67}$$

Written in its component form, the $\underset{\sim}{Z}_c$ matrix is

$$\underset{\sim}{Z}_c = \begin{bmatrix} Z_{11}, Z_{12}, \cdots & \cdots & Z_{1n} \\ Z_{21}, Z_{22} & \cdots & Z_{2n} \\ \vdots & \ddots & \vdots \\ Z_{p1}, Z_{p2} & Z_{pp} \cdots & Z_{pn} \\ \vdots & \ddots & \vdots \\ Z_{n1}, Z_{n2} & \cdots & Z_{nn} \end{bmatrix} \tag{68}$$

Making use of the definition of $\underset{\sim}{P}$, we find from Eqs. (52), (63), (65), and (68):

$$(d\underset{\sim}{Z}_c) = -\, j\, d(\omega C) \begin{bmatrix} (Z_{1p}Z_{p1}), (Z_{1p}Z_{p2}) \cdots & \cdots & (Z_{1p}Z_{pn}) \\ (Z_{2p}Z_{p1}), (Z_{2p}Z_{p2}) \cdots & \cdots & (Z_{2p}Z_{pn}) \\ \vdots \quad \vdots & \ddots & \vdots \\ (Z_{pp}Z_{p1}), (Z_{pp}Z_{p2}), \cdots & Z_{pp}^2, \cdots & (Z_{pp}Z_{pn}) \\ \vdots \quad \vdots & \ddots & \vdots \\ (Z_{np}Z_{p1}), (Z_{np}Z_{p2}) \cdots & \cdots & (Z_{np}Z_{pn}) \end{bmatrix} \tag{69}$$

Eq. (69) shows a basic relation between the change $(d\underset{\sim}{Z}_c)$ in the impedance matrix and the elements of the impedance matrix when the pth gap is perturbed. For a given excitation current vector $\underset{\sim}{I}$, the change in the impedance matrix results in a change $(d\underset{\sim}{V})$ in the gap voltage distribution. This change is

$$(d\underset{\sim}{V}) = (d\underset{\sim}{Z}_c)\ \underset{\sim}{I} \tag{70}$$

The simplest relations are obtained when the resonator is excited at one gap at a time, for example the qth gap. We shall further assume that the gap voltage is measured in the ℓth resonator cell. In this case we get from Eqs. (69) and (70)

$$(dV_\ell)_{pq} = -\,j\ d(\omega C)\ (Z_{\ell p} Z_{pq})\ I_q \tag{71}$$

It should be recalled that the subscript p in Eq. (71) identifies the perturbed cell.

Eq. (71) provides the basis for our measurement method. By selecting several combinations of the values of ℓ, p and q, a sufficient number of equations is obtained to determine all the elements of the circuit matrix.

The total number of elements in the circuit matrix for an n-gap resonator is n^2. The resonator is a passive circuit and therefore the circuit matrix $\underset{\sim}{Z}_c$ is symmetric, i.e.,

$$Z_{rs} = Z_{sr} \tag{72}$$

for any value of r and s. Because this is true, the total number of unknown elements m is reduced to

$$m = \frac{n}{2}(n+1) \tag{73}$$

Therefore, only a small fraction of the possible combinations of values of ℓ, p and q are needed for the determination of the circuit matrix. We shall make use of this to create a simple measurement method.

In an actual measurement it is most convenient to measure the change in the gap voltage in the cell coupled to the external load. The coupling is strong and not easily subject to accidental changes in this case. The value of ℓ will therefore be fixed to the identification number of the loaded cell. The remaining n^2 equations obtained by the possible combination of p and q is still sufficient. Excitation of the different cells can be done with small coupling loops. Care must be taken to avoid detuning of the cell by using small penetrations of the loops into the resonator. The measurement is performed by successive perturbations of the different interaction gaps for each location of the excitation loop.

In order to determine the absolute values of the circuit matrix elements by this measurement method alone, it is necessary to know the absolute values of $(dV_\ell)_{pq}$ and I_q. In addition, the perturber must be calibrated to assign a value to $d(\omega C)$. This is inconvenient. Each of the coupling loops would have to be calibrated, and equations would have to be derived relating the loop currents to the induced gap currents.

However, the excitation currents can be eliminated as unknowns from the set of equations generated by the measurement (Eq. (71)). This also eliminates the need for knowing the value of d(C) and the calibration constant between the gap voltage and voltage across the load (waveguide) in the loaded cell. In this case it is not possible to find all of the matrix elements, but only the ratios of the circuit impedance matrix elements to one of the other matrix elements. However, the value of this reference element, which must be one of the diagonal elements, can be determined by the method described in part C of this section. The total number of equations provided by the measurement (n^2) is still sufficient.

C. Measurement of the Diagonal Elements of the Circuit Impedance Matrix

A method presented by Lakits[6] for finding the interaction impedance of filter-loaded resonators can be used for determining the diagonal elements in the circuit impedance matrix. (See Appendix A of reference 7 for a correction to one of his equations which, however does not change his general conclusions).

In the equivalent circuit of Fig. 9, used in the derivation of the circuit impedance matrix, the external load was represented by a series resistance in the loaded cell of the network. Since coupling to the load port is required for the present measurement, the modified equivalent network shown in Fig. 10 must be used. The circuit is to be assumed lossless (as required by Lakits' assumption) and the load resistance in the ℓth cell is replaced by a more complex coupling circuit. The original n-port network of Fig. 9 is thereby converted into an (n+1)-port network. The voltages at the ports are related to the drive currents by:

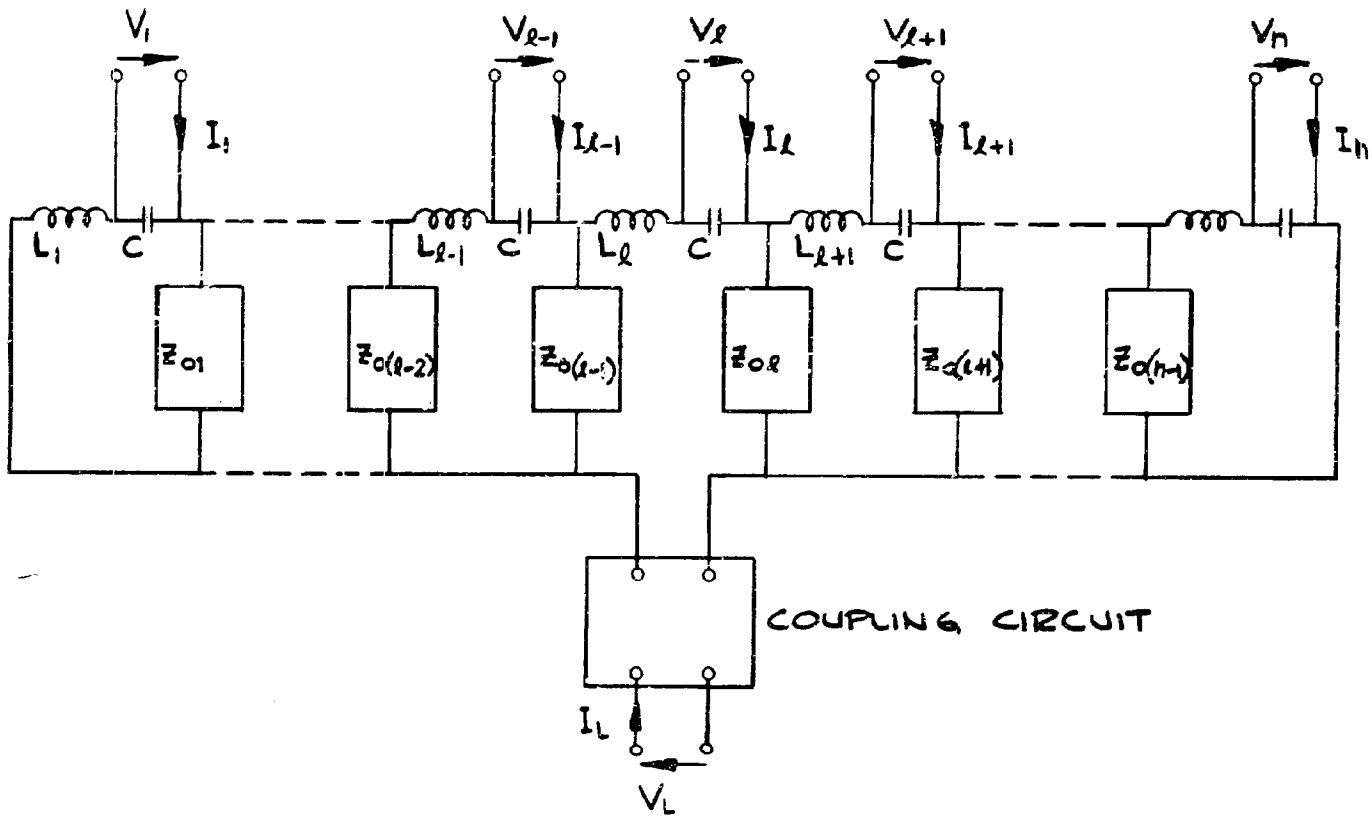

Fig. 10 - Equivalent lumped circuit consisting of n coupled resonators. The circuit is lossless and is coupled to the external load through a coupling circuit in the ℓth network cell.

$$\begin{bmatrix} V_1 \\ V_2 \\ \vdots \\ V_\ell \\ V_p \\ \vdots \\ V_n \\ V_L \end{bmatrix} = \begin{bmatrix} Z_{11}, Z_{12} & \cdots & Z_{1n}, Z_{1L} \\ Z_{21}, Z_{22} & \cdots & Z_{2n}, Z_{2L} \\ \vdots & \ddots & \vdots \\ Z_{L1}, Z_{L2} & \cdots & Z_{LL} \end{bmatrix} \begin{bmatrix} I_1 \\ I_2 \\ \vdots \\ V_\ell \\ I_p \\ \vdots \\ I_n \\ I_L \end{bmatrix} \qquad (78)$$

The coupling circuit is designed to simulate the loading of the original circuit at all frequencies of interest. When the Lth port is loaded with the characteristic impedance of the waveguide, all the elements Z_{rs} for $1 < r < n$ and $1 < s < n$ in Eq. (78) are equal to the equivalent element of the circuit impedance matrix of the original circuit.

In order to conform to the concepts used by Lakits, the capacitive perturbation of one of the interaction gaps of the circuit must be considered as the connection of a parallel susceptance $\Delta(\omega C)$ to the gap. We shall assume that we are perturbing the pth gap and are exciting the resonator through the load port L. In this case all the gap currents except I_p and I_L are zero. The currents and the voltages at the Lth and pth ports are now interrelated by

$$\begin{bmatrix} V_p \\ V_L \end{bmatrix} = \begin{bmatrix} Z_{pp} & Z_{pL} \\ Z_{Lp} & Z_{LL} \end{bmatrix} \begin{bmatrix} I_p \\ I_L \end{bmatrix} \tag{79}$$

By using simple transformation rules this equation can be transformed into the two-port network representation used by Lakits.

$$\begin{bmatrix} V_p \\ I_p \end{bmatrix} = \begin{bmatrix} A & B \\ C & D \end{bmatrix} \begin{bmatrix} V_L \\ -I_L \end{bmatrix} \tag{80}$$

A direct application of Lakits' method will yield the value of the self impedance Z_{pp} of the pth interaction gap. All the diagonal elements of the impedance matrix can therefore be found by this method.

CONCLUSIONS AND FUTURE PLANS

A. Conclusions

A discussion was presented showing that by a proper selection of resonator parameters, the frequency response of two-gap extended-interaction resonators with overlapping modes can be made quite insensitive to changes in the beam voltage. One example case was cited wherein the beam voltage could be varied over a range of approximately fifty percent without seriously affecting the resonator's frequency response curve or its bandwidth.

A complete set of equations have been derived for computing the small-signal gain and phase vs. frequency response of klystrons which employ extended-interaction resonators with overlapping modes. These equations are being programmed for a digital computer. The gain equation is written as a determinant of matrices, and the elements of the matrices will be calculated within the computer program. The elements of the circuit admittance matrix of each resonator will be computed from the equivalent-circuit parameters of the resonators, and the elements of the electronic admittance matrices will be computed from the beam and gap parameters. While the equations were derived for the particular case of klystrons containing only two-gap extended-interaction resonators or single-gap resonators, the method is generally applicable to resonators with any number of gaps, including multiple-tuned single-gap resonators.

The theoretical basis for a cold-test method applicable to extended-interaction resonators with overlapping modes and to filter-loaded resonators has been developed. By using this method, all of

the elements of the resonator's circuit impedance matrix can be measured, and the characteristics of the resonator completely determined. The off-diagonal elements of the matrix can be evaluated relative to one or more of the diagonal elements. The values of the diagonal elements can be measured directly.

B. Future Plans

The writing of the small-signal gain-bandwidth computer program will be completed, and computations will be started. At first, the input resonator will be studied independently to see whether the generator should be coupled to the first cavity or the second cavity, or whether it could be coupled to either with equal results. Once that has been done, small-signal calculations will be carried out for the entire buncher section. Initially, all of the buncher resonators will be designed for full-band coverage (except for the penultimate resonator system which must be tuned outside the frequency band). The relatively-high interaction impedance which can be expected from resonators with mode overlapping indicates that this approach is feasible.

The cold-test method described in this report will be evaluated experimentally by first applying it to single-mode resonators. The results obtained can then be compared with measurements made using conventional techniques. Following this, the cold testing of two-gap extended-interaction resonators with overlapping modes will be started.

A computer program for the large-signal analysis of extended-interaction resonators with overlapping modes will be developed. The

program will be capable of simulating and accounting for the remodulation of the beam within a multi-gap resonator, and will be used for the final evaluation of output resonators.

An over-all tube design will be formulated from the combined results of the large-signal analysis, the small-signal analysis, and the cold-test measurements.

REFERENCES

1. E. Lien, D. Robinson, "Study and Investigation Leading to the Design of Broadband High-Power Klystron Amplifiers", Technical Report No. ECOM - 02157-1, March, 1967.

2. Ibid, pp. 3-40.

3. T. Wessel-Berg, "Space-Charge Wave Theory of Interaction Gaps and Multi-Cavity Klystrons with Extended Fields", Norwegian Defense Research Establishment, Bergen, Norway, Report No. 32; 1960.

4. E. Lien, D. Robinson, "Study and Investigation Leading to the Design of Broadband High-Power Klystron Amplifiers", Technical Report No. ECOM - 01362-1, November, 1965, pp. 6,7.

5. T. Wessel-Berg, op. cit., pp. 81-91.

6. E. Lakits, "Measurements of the Interaction Impedance of a Klystron Broadband Coupling Circuit", IRE Wescon Convention Record, Session 27/2, 1961.

7. E. Lien, D. Robinson, "Study and Investigation Leading to the Design of Broadband High-Power Klystron Amplifiers", Technical Report No. ECOM - 01362-F, November, 1966, Appendix A.

GLOSSARY OF SYMBOLS

A	Amplitude of the current I_1 (except in Eq. (80), where A is an element of the A,B,C,D-parameter matrix)
a_2	Amplitude coefficient of the current I_2 ($\|I_2\| = a_2 A$)
c	Free-space velocity of light
C	Cavity interaction-gap capacitance (except in Eq. (80), where C is an element of the A,B,C,D-parameter matrix)
$\underset{\sim}{C}$	Interaction-gap-capacitance matrix, defined by Eq. (52)
e	Electronic charge
$G_{e,sn}$	Beam-loading conductance of the nth gap in the sth resonator, defined by Eq. (18)
i	Circulating cavity current
$\underset{\sim}{i}$	Circulating cavity current vector, defined in Eq. (50,
I_o	DC beam current
I	Induced gap current
I_1, I_2	Induced rf currents in the first and second gaps of a two-gap resonator
I_g	RF current from the generator
I_{sn}	In Eqs. (10) through (48), the rf current induced in the nth gap of the sth resonator
$\underset{\sim}{I}$	Induced gap current vector, defined in Eq. (50)
j	$\sqrt{-1}$
$\underset{\sim}{K}$	Impedance matrix, defined by Eq. (53)
ℓ	In Eqs. (49) through (80), denotes the gap within the resonator at which the voltage is being measured in cold test
$\ell_{sn,rm}$	In Eqs. (10) through (48), axial distance from the center of the mth gap of the rth resonator to the center of the nth gap of the sth resonator
L_o	Coupling inductance between cavities

L	Cavity inductance (except in Eqs. (78) through (80), where it denotes the load port of a multi-gap resonator)
L_1, L_2	Equivalent inductances of the cavities in a two-gap resonator
m_o	Electron rest mass
m	In Eqs. (10) through (48), a subscript denoting one of the gaps of a resonator
m	In Eqs. (49) through (80), the total number of unknown elements in the matrix $\underset{\sim}{Z}_c$
M^-	Gap coupling coefficient of the fast space-charge wave, defined in Eq. (19)
M^+	Gap coupling coefficient of the slow space-charge wave, defined in Eq. (20)
n	In Eqs. (10) through (48), a subscript denoting one of the gaps of a resonator
n	In Eqs. (49) through (80), the total number of gaps within the resonator
p	In Eqs. (2) and (3), the spacing between the centers of the gaps in an extended-interaction resonator
p	In Eqs. (10) through (48), the total number of resonators in the klystron
p	In Eqs. (49) through (80), denotes which gap is being perturbed within the resonator in cold test
P_a	Power available from the generator
P_{out}	Average rf power dissipated in the klystron load
P_p	Average rf power delivered from the beam to the pth resonator
$\underset{\sim}{P}$	A matrix with all elements equal to zero except the pth diagonal element, which is unity
q	In Eqs. (49) through (80), denotes the gap within the resonator which is being excited in cold test
Q_1, Q_2	Total loaded Q values of the cavities in a two-gap resonator, measured before the cavities are coupled together
Q_{ext}	External Q

$(Q_{ext})_{g,1n}$	That part of the external Q of the nth cavity of the input resonator associated with the coupling to the generator
r	In Eqs. (10) through (48), a subscript denoting an arbitrary resonator occuring before the sth resonator ($r \leq s$)
r	In Eqs. (49) through (80), denotes an arbitrary subscript within the matrix $\underset{\sim}{Z}_c$
R	Cavity series resistance
R_c	Relativistic correction factor, defined by Eq. (5)
R_g	Effective internal impedance of the generator
R_{sh}	Equivalent cavity shunt resistance
R_{sh}/Q	Characteristic impedance-quality-factor of a cavity
s	In Eqs. (10) through (48), a subscript denoting an arbitrary resonator occuring past the rth resonator ($s \geq r$)
s	In Eqs. (49) through (80), denotes an arbitrary subscript within the matrix $\underset{\sim}{Z}_c$
S	Voltage standing-wave ratio (VSWR)
u_o	DC beam velocity
V_o	DC beam voltage
V_g	Generator voltage
V_{sn}	In Eqs. (10) through (48), the rf voltage on the nth gap of the sth resonator
$\underset{\sim}{V}$	Gap voltage vector, defined by Eq. (49)
$\underset{\sim}{V}_1$	Gap voltage vector of the input resonator
$\underset{\sim}{V}_p$	Gap voltage vector of the pth resonator, defined by Eq. (10)
$Y_{s2,s1}$	Electronic transfer admittance from the first to the second gap of the sth two-gap resonator, defined by Eq. (21)
$Y_{sn,rm}$	Electronic transfer admittance from the mth gap of the rth resonator to the nth gap of the sth resonator, defined by Eq. (23)
$\underset{\sim}{Y}_{c,s}$	Circuit admittance matrix of the sth resonator, defined in Eq. (15)

$\underset{\sim}{Y}_{e,s}$	Electronic admittance matrix of the sth resonator, defined by Eq. (16)
$\underset{\sim}{Y}_{s,s}$	Self-admittance matrix of the sth resonator, defined by Eq. (14)
$\underset{\sim}{Y}_{s,r}$	Electronic transfer-admittance matrix between the rth and the sth resonators, defined by Eq. (22)
Z_i	Input impedance of the input resonator as seen by the generator, defined by Eq. (30)
Z_{op}	Impedance of the coupling element between the pth and (p+1)th cells of the resonator (see Fig. 9)
Z_p	Series impedance of the pth resonator cell, defined by Eq. (54)
Z_{rs}	In Eqs. (49) through (80), one of the elements of the circuit matrix $\underset{\sim}{Z}_c$
$Z_{sn,rm}$	Elements of the matrix $\underset{\sim}{Z}_{s,s}$
$\underset{\sim}{Z}_c$	Circuit impedance matrix, defined by Eq. (57)
$\underset{\sim}{Z}_{s,s}$	Inverse of the matrix $\underset{\sim}{Y}_{s,s}$
α	L_o/L_1
β_2	L_2/L_1
β_e	Propagation factor associated with the dc beam velocity ($\beta_e = \omega/u_o$)
$\beta_e p$	In Eqs. (2) and (3), normalized spacing between the centers of the gaps in an extended-interaction resonator
β_q	Plasma propagation factor ($\beta_q = \omega_q/u_o$)
γ_2	ω_2/ω_1
$\underset{\sim}{\eta}_{s,r}$	Voltage-gain matrix of the rth and sth resonators with the intermediate resonators removed, defined by Eq. (13)
θ_2	Phase of I_2 relative to I_1
ρ	Voltage reflection coefficient
ϕ	Total voltage phase shift through the klystron
ω	Angular frequency

ω_1, ω_2	Angular resonant frequencies of the cavities in a two-gap resonator before they are coupled together
ω_n	Angular frequency of the nth mode, at which the cavity parameters were measured (Fig. 1 and Fig. 5)
ω_q	Reduced angular plasma frequency

Security Classification

DOCUMENT CONTROL DATA - R & D

(Security classification of title, body of abstract and indexing annotation must be entered when the overall report is classified)

1. ORIGINATING ACTIVITY (Corporate author)
Varian Associates
EIMAC Division
301 Industrial Way, San Carlos, California 94070

2a. REPORT SECURITY CLASSIFICATION
Unclassified

2b. GROUP

3. REPORT TITLE
Study and Investigation Leading to the Design of Broadband High Power Klystron Amplifiers

4. DESCRIPTIVE NOTES (Type of report and inclusive dates)
Second Triannual Report, 10 December 1966 to 9 April 1967

5. AUTHOR(S) (First name, middle initial, last name)
E. Lien and D. Robinson

6. REPORT DATE	7a. TOTAL NO. OF PAGES	7b. NO. OF REFS
July 1967	51	7

8a. CONTRACT OR GRANT NO.	9a. ORIGINATOR'S REPORT NUMBER(S)
DA 28-043 AMC-02157 (E)	
b. PROJECT NO. 1E6-22001-A-055-04-78	
c.	9b. OTHER REPORT NO(S) (Any other numbers that may be assigned this report)
d.	ECOM-02157-2

10. DISTRIBUTION STATEMENT
This document is subject to special export controls and each transmittal to foreign governments or foreign nationals may be made only with prior approval of CG, USAECOM, Attn: AMSEL-KL-TM, Fort Monmouth, New Jersey 07703.

11. SUPPLEMENTARY NOTES	12. SPONSORING MILITARY ACTIVITY
	U. S. Army Electronics Command Fort Monmouth, New Jersey 07703

13. ABSTRACT
See Attached Sheet

DD FORM 1473 (1 NOV 65) REPLACES DD FORM 1473, 1 JAN 64, WHICH IS OBSOLETE FOR ARMY USE

Security Classification

14 KEY WORDS	LINK A		LINK B		LINK C	
	ROLE	WT	ROLE	WT	ROLE	WT
Broad Band Klystron Extended Interaction Mode Overlapping						